sciendo INTERNATIONAL JOURNAL ON SMART SENSING AND INTELLIGENT SYSTEMS

Article | DOI: 10.2478/ijssis-2023-0011 Issue 1 | Vol. 16 (2023)

Performance Evaluation of ST-Based Methods for Simulating and Analyzing Power Quality Disturbances

Husham I. Hussein[1,2], Ahmed Alazawi[1,2], A. Rodríguez[1,*] and F. Muñoz[1]

[1]Electrical Engineering Department, University of Malaga, Dr Ortiz Ramos s/n, 29071- Malaga, Spain

[2]Electrical Power &Machines Department, College of Engineering, University of Diyala. Diyala. Iraq

*E-mails: 0611056898@uma.es; 0611056851@uma.es; arodriguezg@uma.es; fjmg@uma.es

Received for publication August 11, 2023.

Abstract

The complexity of power quality disturbances (PQDs) is a significant risk factor in the electricity sector. An accurate and fast analysis of these disturbances provides crucial information to cover all the issues related to power quality. The main objective of this study is to explore a new analytic technique, including all kinds of disturbances that can appear in electrical networks, that differs from previous technologies such as the Fourier transform. Three methods based on the Stockwell transform, namely, the discrete orthonormal Stockwell transform (DOST), discrete cosine Stockwell transform (DCST), and discrete cosine transform (DCT), were used to analyze PQDs in time–frequency representation. These methods diagnose the disturbance's signal properties, which are dependent on resolution and absolute phase information. Nine PQDs, including normal sine waves, were mathematically modeled and used to evaluate the proposed methods. All the methods can effectively simulate and analyze PQDs. Among them, DOST is the most effective in providing clear and high-resolution time–frequency representations of signals. The classification of disturbances was fulfilled based on statistical features extracted from matrices derived from Stockwell transform-based methods, such as analytic approaches (mean, variation, standard deviation, entropy, skewness, and kurtosis). Neural networks, a method utilizing intelligence classifiers, were used for pattern recognition, and the patterns of the different methods were compared. Simulation results proved that DOST needs fewer samples than other methods; its capability to deal with signals in time–frequency resolution is also more viable. The neural network classifier has a higher accuracy rate than the K-nearest neighbor and decision tree methods and approximates the support vector machine method.

Keywords

DOST, DCST, DCT, time–frequency, power quality disturbance, signal processing

1. Introduction

With the emergence of modern power systems, the severity of supply power quality problems has increased due to the proliferation of disruptive resources, such as nonlinear loads and renewable energy. In an attempt to address these issues and take advantage of safe time, increased accuracy, and fast response and analysis, the provision of information about the disturbances is of utmost importance.

Open Access. Published by Sciendo. CC BY-NC-ND
© 2023 Hussein et al. This work is licensed under the Creative Commons Attribution-NonCommercial-NoDerivs 4.0 License https://creativecommons.org/licenses/by-nc-nd/4.0/

Many methods and algorithms are currently employed to achieve a high level of analysis and extract the disturbance information. The Stockwell transform, introduced in Ref. [1], is an effective tool for the time–frequency resolution analysis of power quality disturbance (PQD) signals. The Stockwell transform operates by fixing the modulating ability with respect to the x-axis (time axis), while the localized scalable Gaussian window handles dilation and translation. This interrelation results in a phase spectrum that is absolute and always referenced to the origin of the time axis, which serves as a fixed reference point. Previous studies [2, 3] have explored the detection, classification, and localization of PQDs using various types of wavelet functions and consequently have provided time and frequency information by means of multi-resolution analysis. However, the wavelet transform is limited in its ability to analyze nonstationary signals; this aspect is where the Stockwell transform proves its capabilities. In Ref. [4], the Stockwell transform was introduced for PQD analysis by using parameters such as root mean square (RMS; instantaneous and fundamental RMS), total harmonic distortion (THD), TnHD, and total waveform distortion of the disturbances. A comparison study [5] between the Stockwell transform, wavelet transform (WT), and short-time Fourier transform (STFT) was also proposed for power quality analysis. The discrete orthonormal Stockwell transform (DOST) has been illustrated as having a clear structure [6, 7]. From the DOST concept, the discrete cosine transform (DCT) and discrete cosine Stockwell transform (DCST) were derived, both of which can produce real-valued transforms. The properties of these transforms, including their basis functions and directed graph structures of coefficients, have also been investigated. In Refs [8, 9], DOST and other methods were used to analyze PQDs that may occur in ultrahigh-voltage power system transmission lines caused by faults. For new feature extraction based on DOST, the two-dimensional fast-DOST was proposed [10], and the genetic algorithm (NSGA-II) was employed for the determination task. DOST was also used in Refs [11, 12] to analyze nonstationary signals related to ground motions by using a seed record or target amplitude of DOST coefficients. In Ref. [13], the Wigner–Ville distribution synchronized with the Hilbert transform was considered to specifically analyze the most common PQDs, including sag and swell. The Hilbert transform was employed to convert the data into an analytical format that could be fed into the Wigner–Ville distribution for improved signal processing. The assessment of PQDs further introduced a new trend [14] of applying the synthetic evaluation method for steady-state power quality, incorporating improvements from the traditional best–worst method by using triangular fuzzy numbers. Furthermore, solutions for locating poor power quality sources and fault locations were used to identify the origin of disturbances in the electric network and improve the responsibility assignment [15]. In Ref. [16], the principles of various machine learning techniques were introduced to improve the efficacy and management of power distribution networks. The effectiveness of unsupervised and supervised models was evaluated using various indicators. As a recent field of deep learning, neural networks have been used for PQD classification purposes. Convolutional neural networks were presented in Ref. [17] as detectors and classifiers for faults. In this study, we present nine disturbance signals related to PQDs and analyze them using the aforementioned proposed methods. Performance evaluation was conducted for each disturbance, and the results obtained from DOST, DCST, and DCT were compared. The aim of this research was to evaluate the performance and effectiveness of the proposed methods (DOST, DCST, and DCT) for PQD signal simulation and analysis (stationary and nonstationary). Pattern recognition by neural networks was utilized for intelligence classification-based feature extraction. By utilizing the aforementioned methods, this study can gather insights into the boundaries of traditional power quality analysis approaches, which often rely on methods such as the STFT and WT. The use of Stockwell transform-based methods allows for improved time and frequency localization, providing a more detailed understanding of PQDs. The aforementioned methods can also significantly enhance the detection and localization of PQDs, accurately capturing the time and frequency characteristics of various power quality issues, thereby providing power system operators with a more comprehensive view of system disturbances. Such a level of detail is crucial for promptly diagnosing and addressing power quality problems.

The remainder of this article is organized as follows. Section 2 introduces the materials and methods used in analyzing and classifying PQDs. Section 3 presents the proposed methodology and flowchart. Section 4 discusses the analyses and simulation results of the PQDs obtained from the Stockwell transform-based methods and their corresponding time–frequency representations

(DOST, DCST, and DCT). Cases and examples are provided to verify the effectiveness of the proposed methods subjected to many PQD signals. Section 5 presents the classification of PQDs. The conclusions are presented in Section 6.

2. Materials and methods

The succeeding sections discuss the different time–frequency representations based on Stockwell transform methods that were used for power quality analysis. Neural network classifiers were utilized to classify the disturbances and extracted features into classes. The methods included DOST, DCT, and DCST.

2.1 DOST

In Ref. [18], DOST is presented as a highly effective illustration of the Stockwell transform. The DOST technique represents an orthogonal approach to essential tasks, prioritizing the spectrum and focusing and preserving the valuable phase properties of the Stockwell transform; thus, it can also be viewed as a variation of the Fourier transform. By capitalizing on the concept of low frequencies over longer periods, the DOST allows for the occurrence of relatively low sampling rates, resulting in subsamples that can mainly capture low-frequency components. Conversely, high frequencies necessitate high sampling rates to ensure the proper distribution of coefficients; a sample spacing paradigm is described in Ref. [19]. The DOST offers a collection of (N) orthonormal unit-length vectors that operate within specific regions in the frequency domain, thus providing a versatile set of tools. These districts are stated by three different limitations, namely, *v*, β, and τ. The k_{th} basis vector is given as follows:

$$D[K]_{V,\beta,\tau} = \frac{e^{i\pi\tau}}{\sqrt{\beta}} \sum_{f=V-\frac{\beta}{2}}^{V+\frac{\beta}{2}-1} \exp\left(-i\frac{2\pi}{N}kf\right)\exp\left(i\frac{2\pi}{\beta}\tau f\right) \quad (1)$$

$$S_{V,\beta,\tau} = \left\langle D[K]_{V,\beta,\tau}, h[k]\right\rangle = \frac{1}{\sqrt{\beta}} \sum_{f=V-\frac{\beta}{2}}^{V+\frac{\beta}{2}-1} \exp(-i\pi\tau)\exp\left(i\frac{2\pi}{\beta}\tau f\right)H[f] \quad (2)$$

Thus, DOST is the inner product between a time series h[k] and the basis functions defined as a function of D[*k*], where *v* is the center frequency band for each product, β is bandwidth, and τ is time location.

2.2 DCT

The DCT is based on the discrete Fourier transform but uses real numbers (R). The Stockwell transform represents a collection of data points as the sum of sine wave components with different frequencies (Hz) and amplitudes. In contrast to the complex exponentials used in the Fourier transform, DCT employs cosine functions. The advantages of using DCT include its ability to concentrate most of the data into a few transformed coefficients, its independence from the input data, and its suitability for interpreting frequency-related coefficients. In Ref. [20], DCT was used to extract features that are primarily related to temporal variations. For a one-dimensional signal x(n) of length N, the DCT coefficients X(k) can be calculated as follows:

$$X(K) = \sqrt{\frac{2}{N}} * C(K) * \sum_{n=0}^{N-1}\left\{X(n) * \cos\left[\frac{\pi}{2N} * K * (2n-1)\right]\right\} \quad (3)$$

where X (k) represents the DCT coefficient at index k, C (k) is a scaling factor defined as C(k) = 1 for k = 0, and C(k) = √2 for k ≠ 0.

2.3 DCST

DCT, which is used in many applications during signal processing, is a real-valued transform and hence is better suited for compression and filtering. The use of relations in the Fourier transform contributes to the easy adaptation of the DOST algorithm. The DCT uses only positive frequencies [21]. In DCT, relatively high frequencies are needed, and the frequency space must be partitioned to be adjusted. Furthermore, the most straightforward approach in DCT is to continue using the dyadic partitions.

$$\text{DCST} = \left(\bar{\oplus}_{l=1}^{K}\text{DCT}_{ni}^{-1}\right)\text{DCT} \quad (4)$$

2.4 Pattern recognition based on neural networks

Neural networks are pivotal assets in artificial intelligence (AI) technologies as they can showcase

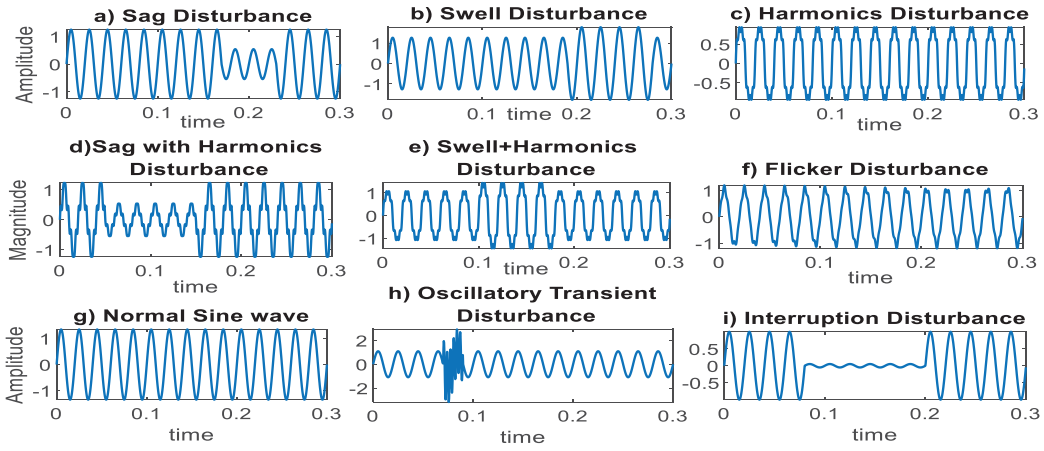


Figure 1: PQD signal models covering all types of disturbance signals (stationary and nonstationary) included normal sine waves.

Table 1. Mathematical models for PQDs and relevant parameters.

PQ disturbance	Class	Equations	Parameters
Normal voltage	C0	$v(t) = A\{1 \pm \alpha[u(t_2) - u(t_1)]\}\sin(\omega t)$	$\alpha < 0.1$
Sag	C1	$v(t) = A\{1 - \alpha[u(t_2) - u(t_1)]\}\sin(\omega t)$	$0.16 \le \alpha \le 0.23$
Swell	C2	$v(t) = A\{1 + \alpha[u(t_2) - u(t_1)]\}\sin(\omega t)$	$0.2 \le \alpha \le 0.28$
Interruption	C3	$v(t) = A\{1 - \alpha[u(t_2) - u(t_1)]\}\sin(\omega t)$	$0.075 < \alpha \le 0.2$
Harmonics	C4	$v(t) = A\sin(\omega t) + h_3\sin(3\omega t)[u(t_{3h2}) - u(t_{3h1})] + h_5\sin(5\omega t)[u(t_{5h2}) - u(t_{5h1})] + h_7\sin(7\omega t)[u(t_{7h2}) - u(t_{7h1})]$	$0 \text{ " } h_i \text{ " } 0.15$
Flicker	C5	$f(t) = (1 + \alpha_f sin(\beta_f \omega t))sin(\omega t)$	$\alpha_f = 0.1 - 0.15,\ \beta_f = 5 - 7.5$
Sag with harm	C6	$v(t) = A\{1 - \alpha[u(t_{sag2}) - u(t_{sag1})]\}\sin(\omega t) + h_3\sin(3\omega t)[u(t_{3h2}) - u(t_{3h1})] + h_5\sin(5\omega t)[u(t_{5h2}) - u(t5_{5h1})] + h_7\sin(7\omega t)[u(t_{7h2}) - u(t_{7h1})]$	$0.05 \le \alpha \le 0.15$
Swell with harm	C7	$v(t) = A\{1 + \alpha[u(t_2) - u(t_1)]\}\sin(\omega t) + h_3\sin(3\omega t)[u(t_{3h2}) - u(t_{3h1})] + h_5\sin(5\omega t)[u(t_{5h2}) - u(t_{5h1})] + h_7\sin(\omega t)[u(t_{7h2}) - u(t_{7h1})]$	$0.1 \le \alpha \le 0.18$
Oscillatory transient	C8	$v(t) = A\sin(\omega t) + \beta\exp[-(t - t_1)/\tau] \cdot \sin[\omega_n(t - t_1)][u(t_2) - u(t_1)]$	$0.1 < \beta < 0.8, 0.066 < \tau < 0.008$ $\omega_n = 2\pi f_n, 500 \le f_n \le 1500$

remarkable competence in fault detection and classification. The efficacy of this technique of using neural networks lies in the existence of an ideal solution for the input data and the nuanced training regimen that defines the system's capabilities [22]. By harnessing the potential of well-calibrated smart systems, the discernment and categorization of power quality disruptions can traverse multiple phases in neural networks. These phases, which are intricately computed via computational analysis, can yield vector matrices. Each matrix serves as the bedrock for executing a robust spectrum of tasks, from anomaly identification to fault categorization, underscoring AI's pivotal role in maintaining seamless power system operations [23]. In this research, pattern recognition based on neural networks was used to classify PQDs.

3. Proposed methodology

The focus of this research was the stationary and nonstationary PQD waveforms, which were normalized based on pure 50 Hz sine wave calculation (Eq. (5)). The disturbance signal *F(t)* is a function of time, with amplitude A and a fixed frequency *f* of 50 Hz denoting the normal power supply voltage frequency. Predefined parameters were adopted for the remaining variables of the PQD model. Figure 1 shows the PQD signals used to meet the objective of this work. Nine disturbance signals were used, including normal sine waves. Table 1 presents the full details of each parameter. Each signal differed in duration. All of the PQDs were modeled and generated using the MATLAB package. After the data for all disturbances were prepared, the data quality was enhanced by pre-processing. This step involved cleaning, transforming, and organizing raw data into a suitable format for further analysis. Figure 2 shows the flowchart of the proposed method, particularly the analysis and classification of the PQDs. Then, the disturbance models were inputted into the Stockwell transform-based methods (DOST, DCST, and DCT). The signals in the time–frequency representation were analyzed, and the matrices for all types of PQDs were obtained. Features were extracted for each signal, including the mean, variation, standard deviation, entropy, skewness, and kurtosis. The technique of recognizing patterns by using neural networks was employed to classify the disturbance based on the derived features.

$$F(t) = A\sin(2\pi ft) \tag{5}$$

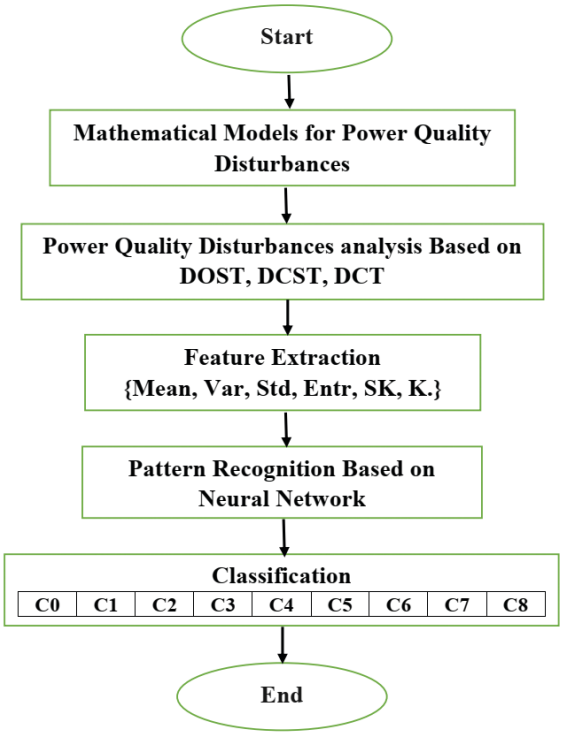


Figure 2: Flowchart of the PQD analysis and classification system.

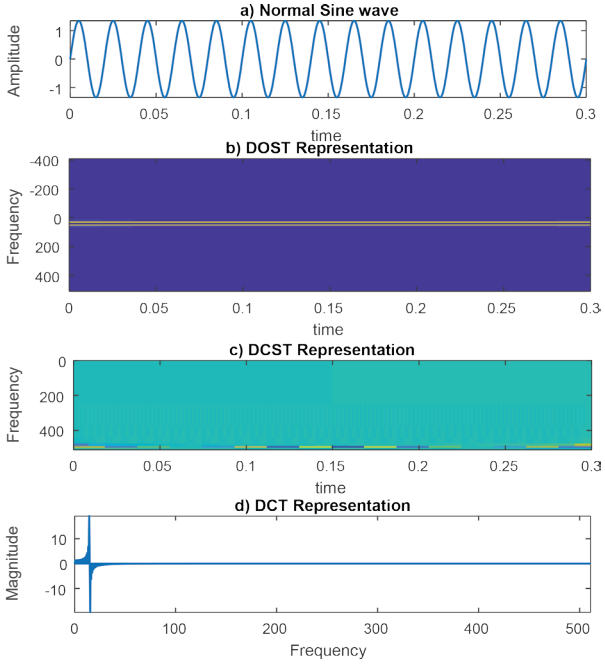


Figure 3: Normal sine wave: (a) target disturbance – nonstationary signal (clean and stable sine wave without any disturbance) for all methods, (b) DOST, (c) DCST, and (d) DCT.

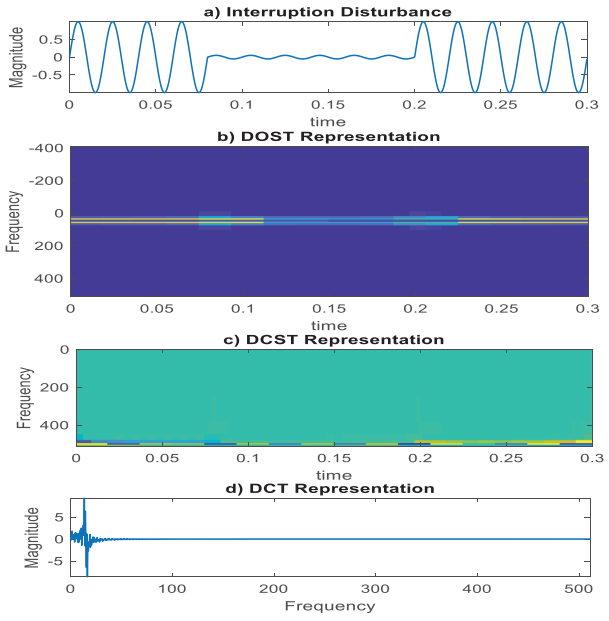


Figure 4: Interruption disturbance signal: (a) target disturbance – nonstationary signal (from 0.075 s to 0.2 s) for all methods. Intended coefficients of the time and frequency fluctuations, including amplitude and angle, for all methods; (b) DOST – the signal time interval corresponds to the target signal and works to accurately capture localized changes in signal characteristics; (c) DCST – some effects on the windows; and (d) DCT – much more limited frequency resolution compared with other time–frequency analytic methods but may capture a few fine-frequency details in the PQDs.

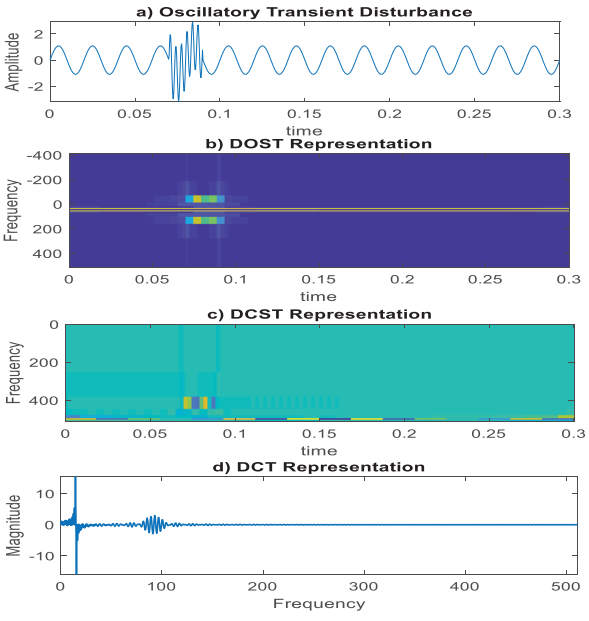


Figure 5: Oscillatory transient disturbance signal: (a) target disturbance – nonstationary signal and its corresponding Stockwell transform-based methods, in which disturbance in all plots occurs at 0.066–0.08 s; (b) DOST – may exhibit better noise robustness than other time–frequency analytic techniques, resulting in cleaner and clearer plotting of PQDs even in the presence of noise or interference; (c) DCST – frequency magnitude increased to 400 Hz corresponding to the time disturbance interval in (b); and (d) DCT – rising multiples in these disturbances, from 0 Hz to 105 Hz, with inter-harmonic and harmonic features.

4. Simulation and analytical results

In this study, three methods based on the Stockwell transform were employed to achieve the proposed purpose of analyzing DOST, DCST, and DCT. The goal of our performance evaluation was to demonstrate whether these methods could deliver high-accuracy performance in the time–frequency representation. These techniques can quickly reveal the quality of events and entail excellent and clear contrasting features and high frequencies, enabling us to determine the locations, times and intervals of failures, and the interruptions and distortions occurring in power system networks (power quality issues). The sampling can handle low-ratio information by mixing low-frequency and high-interval data. Here, DOST was considered a derivative of the Fourier transform, acting as a submodel for low frequencies. The scheme can handle high-frequency data by taking specific samples and distributing them with interspaces. It also provides vectors for all lengths of orthogonal units within the time–frequency representation. Then, DCST (i.e., DOST based on DCT) was used for high-frequency data to achieve high-resolution results. The disturbance signals were simulated with different time periods to facilitate the study of the capabilities of all methods. Figures 3–5 show the simulation results for the nonstationary disturbance signals (normal sine wave, interruption, and oscillatory transient) in DOST, DCST, and DCT as

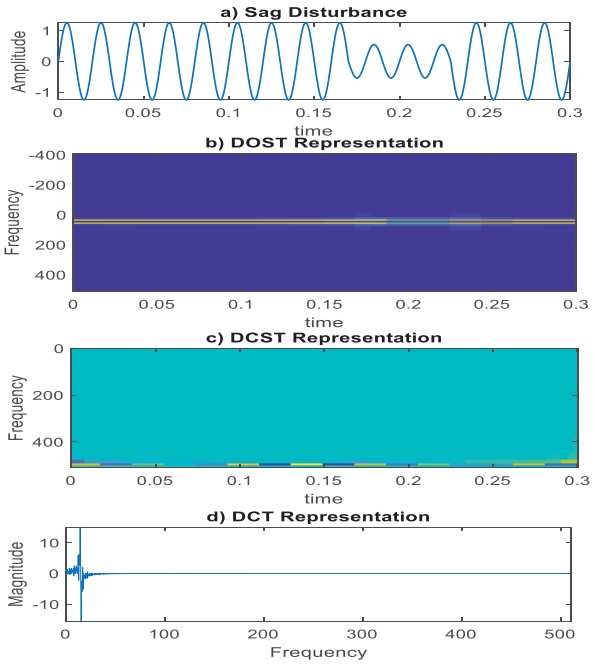


Figure 6: Sag disturbance signal: (a) target disturbance – stationary signal and its corresponding plots allow each method to perform excellently, with the disturbance occurring from 0.16 s to 0.23 s; the intended coefficients of both time and frequency fluctuations, including amplitude and angle, for all methods. (b) DOST – sag effects with a corresponding rate of 100%. (c) DCST – moderate resolution may not capture all of the fine details for certain PQDs with rapidly changing characteristics, leading to less clear plots. (d) DCT – operates on discrete data points and assumes the signal to be periodic; this discrete nature may lead to artifacts in the time–frequency representation, affecting the clarity of the plots.

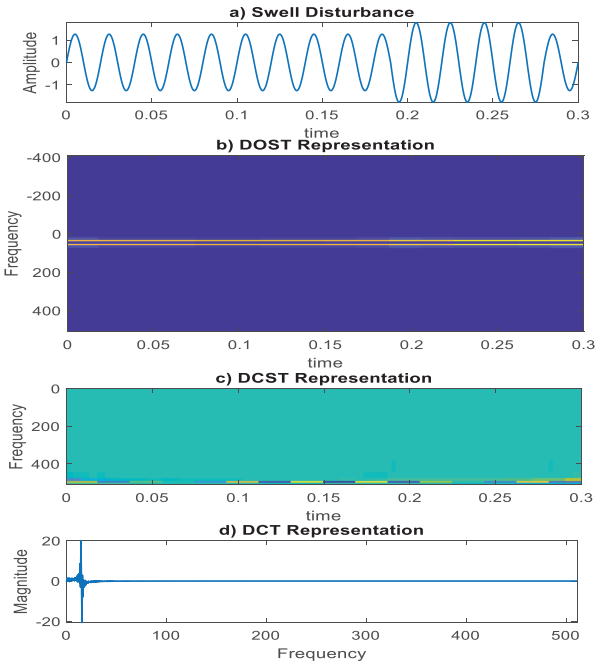


Figure 7: Swell disturbance signal: (a) target disturbance – a stationary signal and represented by all methods, with disturbance occurring from 0.2 s to 0.28 s; the intended coefficients of both time and frequency fluctuations, including amplitude and angle, for all methods. (b) DOST, (c) DCST, and (d) DCT – depend on the specific characteristics of the simulated PQDs. For disturbances with complex or rapidly changing time–frequency components, the DCT may not be the most suitable method, despite its simple but precise plots.

one-dimensional plots with constant amplitudes to represent instantaneous changes in the voltage level. Finally, DCT, which can handle nonnegative frequencies, offers the advantage of being separated into frequency space partitions as a means of inspecting the consequences of different frequencies. Here, no effects appeared with the normal sine wave for all methods, indicating a stable signal with no disturbance. However, for the other forms of disturbances, the effects were evident. In particular, the time period of the disturbance in the time–frequency was at high resolution, especially for the corresponding results with the target signal. Figures 5(b) and 5(c) show the frequency magnitude reaching 400 Hz, which corresponds to the time disturbance interval. This finding implies significant effects starting from 0 Hz to 105 Hz, with the harmonic and inter-harmonic components caused by the strike disturbance. Figures 6–11 show the stationary disturbance signals at different times (i.e., start and end) for each PQD. The methods vary in their effects, which are dependent on the high-frequency content that may have accompanied the disturbances. DOST and DCST demonstrate high levels of representation for the boundary signals, whereas DCT requires more high-frequency content to function properly and

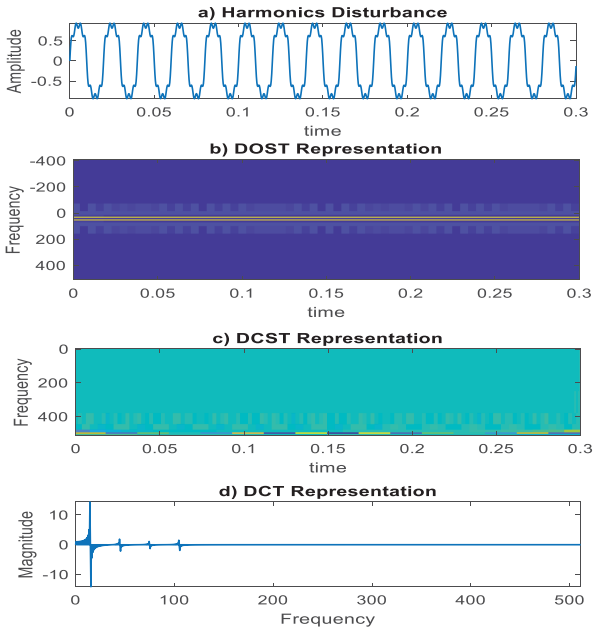


Figure 8: Harmonic disturbance signal: (a) target signal – a stationary signal; the intended coefficients of both time and frequency fluctuations, including amplitude and angle, for all methods. (b) DOST time–frequency representation – ability to represent stationary and nonstationary signals, contributing to the clear plotting of disturbances. (c) DCST time–frequency representation. (d) DCT – known for its energy compaction properties, in which a large portion of the signal energy is concentrated in a few DCT coefficients; this method can result in some aspects of the disturbances being well represented, while others are not.

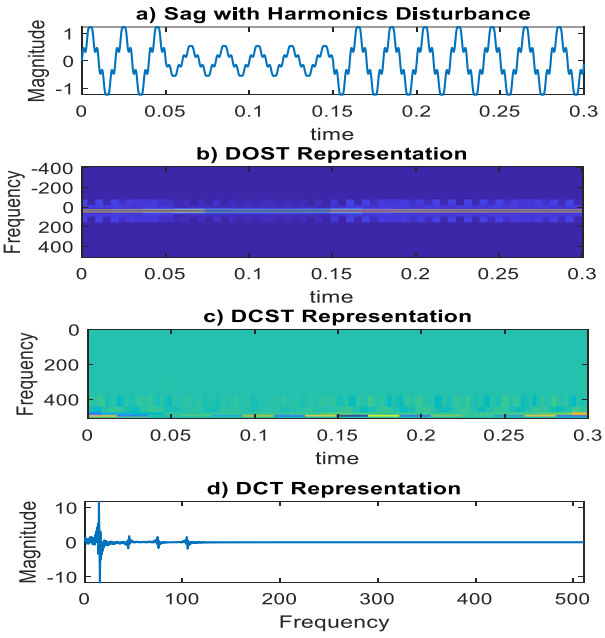


Figure 9: Sag with harmonics disturbance signal: (a) target signal – a stationary signal (from 0.05 s to 0.15 s); the intended coefficients of both time and frequency fluctuation, including amplitude and angle, for all methods. (b) DOST representation – uses different windowing functions in which a selected appropriate window can enhance the clarity of the plot by minimizing spectral leakage and side lobe effects. (c) DCST representation. (d) DCT representation – the rising multiple effective in this type of disturbance (inter-harmonics and harmonics: 25, 50, 75, and 104 Hz).

provide good results. The analysis of disturbances by using Stockwell transform-based methods can obtain results in high resolution with less time and variation. DCST is similar to DCT but slightly restricted in space. The basic task oscillates from its center due to the sharp (cut-off) window, causing ringing around the boundaries and reducing the time locality, although the extent is less apparent for DOST. Notably, some disturbances may exhibit characteristics of disturbance signal behavior depending on the specific context and duration of the disturbance. Additionally, harmonics appear in both stationary and nonstationary disturbances. The distinction between stationary and nonstationary disturbances is based on the duration and consistency of the disturbance. Our results indicate that a strong disturbance signal at high frequency clearly affects DOST, DCST, and DCT. Meanwhile, at medium frequencies, DOST remains clear and DCST is moderately affected, whereas DCT shows no significant effect (Figures 6 and 7). By contrast, as shown in Figures 8–11, DCT has a better capture function than the other methods.

5. Classification of the PQDS

Various disturbances were utilized as targets to obtain the results. Signal processing methods, such as sag (C1), swell (C2), interruption (C3), harmonics (C4), flicker (C5), oscillatory transient (C6), sag with harmonics (C7), and swell with harmonics (C8), were

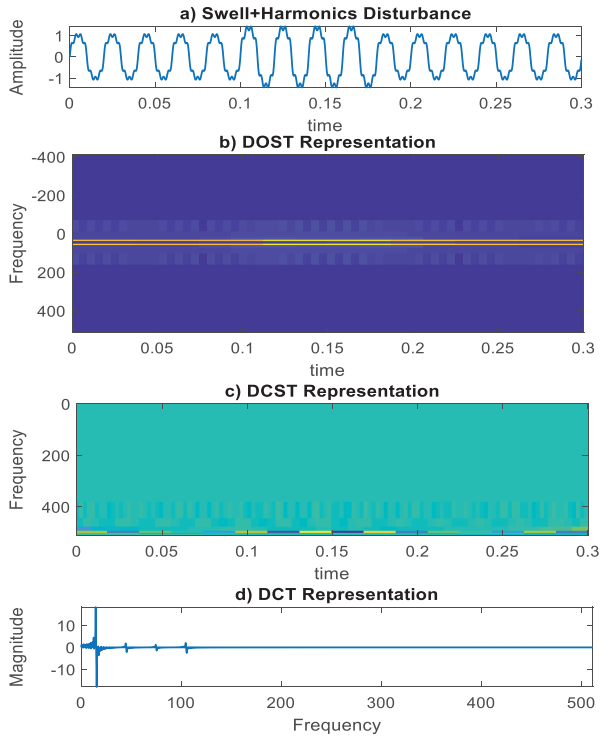


Figure 10: Swell with a harmonic disturbance signal: (a) target signal – a stationary signal from 0.1 s to 0.18 s; the intended coefficients of both time and frequency fluctuation, including amplitude and angle, for all methods. (b) DOST time–frequency representation. (c) DCST representation. (d) DCT representation.

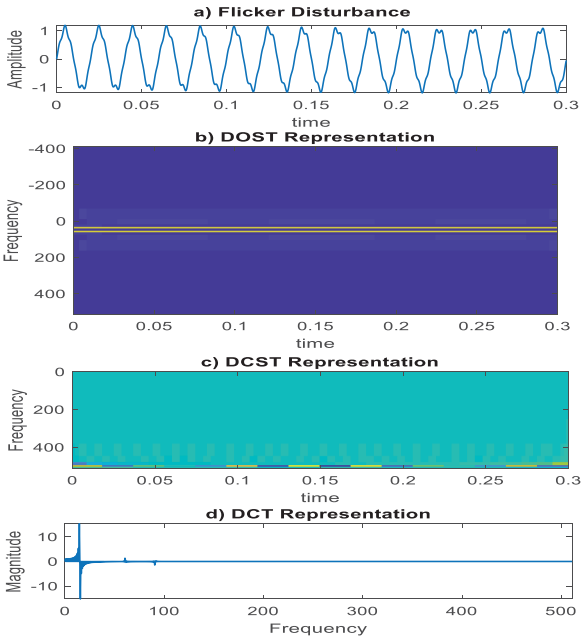


Figure 11: Flicker disturbance signal: (a) original signal – a stationary signal; the intended coefficients of both time and frequency fluctuation, including amplitude and angle, for all methods. (b) DOST, (c) DCST, and (d) DCT – the rising multiple effectiveness in these types of disturbances (25, 75, and 99 Hz for inter-harmonics and harmonics).

used in addition to a normal pure sine wave signal (C0) (Figure 12). The signal properties were as follows: 6.4 kHz as the fundamental frequency, 15 cycles, 128 samples per cycle, and 1920 samples. The value of 100 was set for each case. In this study, a multilayer neural network [24] was used with a three-layer neural network in a forward configuration to form a neural network group. The neural network group employed nine-dimensional feature vectors as inputs and generated a one-dimensional objective output vector. The initial layer comprised nine nodes, followed by a hidden layer with five nodes and an output layer with one node. Each neural network group represented a specific feature category, enabling us to identify distinct disturbance types. In this setup, an output value of 1 signifies the presence of a particular disturbance in the sample, whereas an output value of 0 indicates its absence. This approach could effectively untangle the interconnection between the different disturbance types, further enhancing the recognition accuracy. The signal-to-noise ratio was applied at different levels (20, 30, 40, and 50 dB) to detect the capability of the signal processing methods (DOST, DCST, and DCT) in the disturbance analysis with a distorted environment. The accuracy rate was calculated using three types of methods, namely, decision tree (DT), support vector machine (SVM), and K-nearest neighbor (KNN), in addition to the proposed method of using a neural network. The neural network method outperformed KNN and DT, but SVM obtained a slightly higher accuracy rate (Figure 13). Figure 14 shows that the comparison of the coefficients of the proposed methods – DOST, DCST, and DCT – based on a comprehensive set of statistical properties reveals distinct characteristics of each method. DCT consistently exhibits lower mean values, indicative of its emphasis on preserving the central tendency of the data. However, it also introduces higher variance, skewness, and kurtosis, suggesting increased spread, asymmetry, and heavy tails in distributions. DOST and DCST, on the other

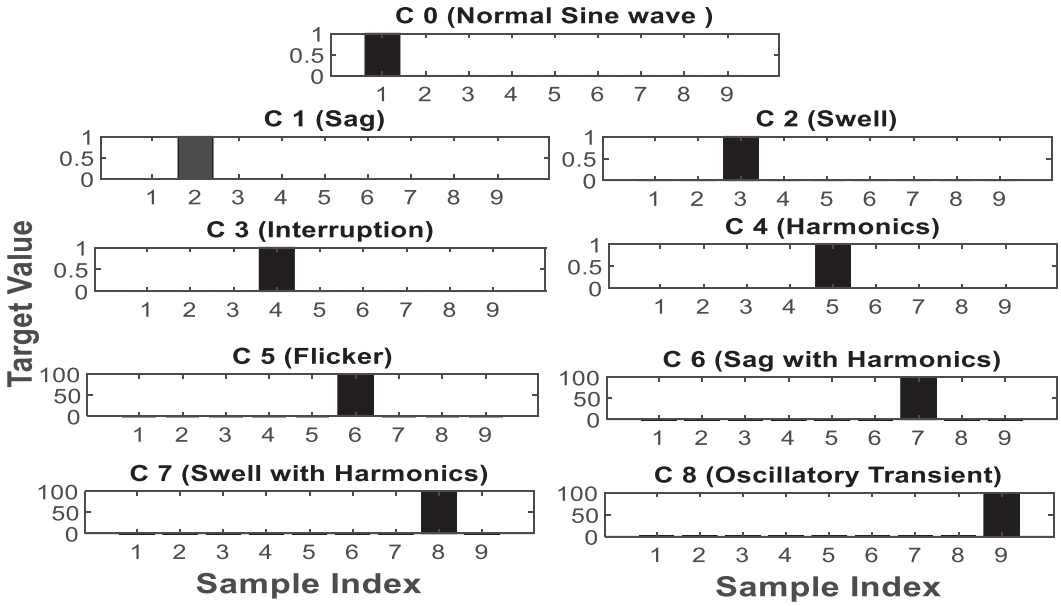


Figure 12: Disturbance classification-based statistical analysis (mean, variation, standard deviation, entropy, skewness, and kurtosis) of the DOST, DCST, and DCT coefficients.

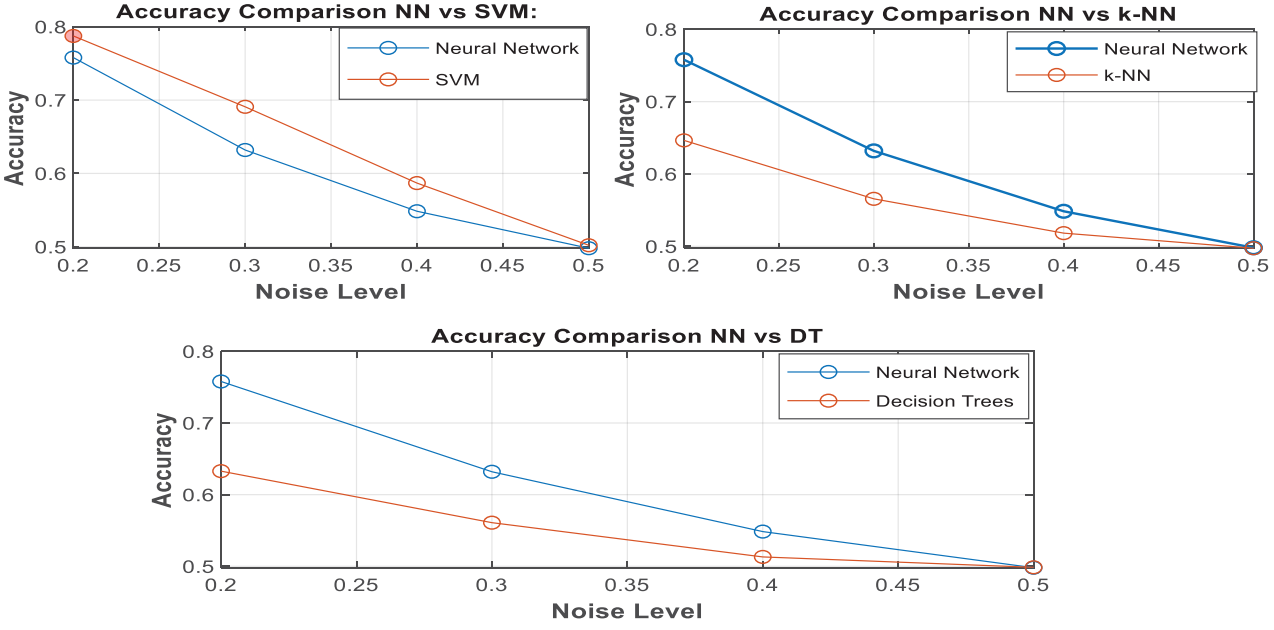


Figure 13: Accuracy comparison between the neural network method and SVM, KNN, and DT.

hand, maintain slightly higher mean values and lower variance, skewness, and kurtosis, implying a propensity for less variation, symmetry, and lighter tails. Standard deviation and entropy measurements confirm DCT's greater spread and lower randomness in data than DOST and DCST. These insights provide valuable guidance for method selection as DCT offers greater variation but might introduce more distortion, while DOST and DCST prioritize data preservation and balance. The choice depends on the application's objectives and preferences regarding data characteristics.

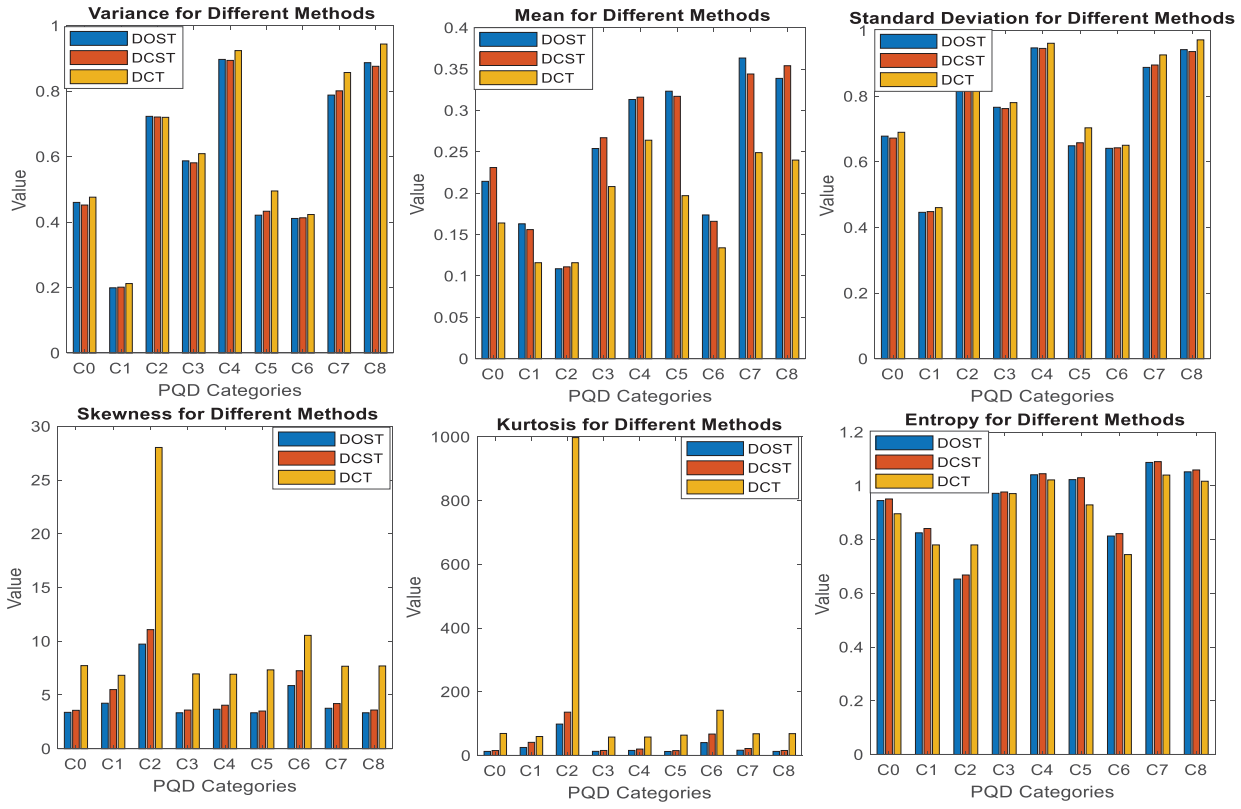


Figure 14: Statistical analysis features properties' comparison (mean, variation, standard deviation, entropy, skewness, and kurtosis) of DOST, DCST, and DCT coefficients.

6. Conclusion

DOST, DCST, and DCT are all signal processing techniques for analyzing and simulating PQDs. The primary difference between these methods lies in the manner in which they transform signals. DOST employs a set of orthonormal basis functions to convert signals into the time–frequency domain, whereas DCST uses cosine functions. Meanwhile, DCT utilizes only cosine functions and is best suited for signals that are symmetric around their midpoint. Regarding their ability to simulate PQDs, each method has its own strengths and weaknesses. DOST appears to be a superior choice because it offers precise and clear representations of signals in the time–frequency domain. DCST is better suited for analyzing harmonic and inter-harmonic distortions, whereas DCT is commonly used for compression applications. Here, the performance of these methods in simulating PQDs was evaluated. The results showed that all three methods can effectively detect and analyze different types of disturbances, but their performances vary depending on the specific characteristics of the signal being analyzed. Therefore, the choice of method depends on the specific application and the type of disturbance being investigated. Regarding the increased values in the performance evaluation, this research found that the neural network classification technique is suitable for classifying PQDs based on the Stockwell transform methods. Matrix vectors extracted from DOST, DCST, and DCT coefficients are inputted into the pattern recognition neural network layers. This technique can be extended to classify a large number of disturbances, and only signal vectors need to be added.

References

[1] P. K. Dash, B. K. Panigrahi and G. Panda, "Power quality analysis using S-transform," in IEEE Transactions on Power Delivery, vol. 18, no. 2, pp. 406–411, April 2003, doi: 10.1109/TPWRD.2003.809616.

[2] M. Gouda, M. M. A. Salama, M. R. Sultan, and A. Y. Chikhani, "Power quality detection and

classification using wavelet multi-resolution signal decomposition," *IEEE Trans. Power Delivery*, vol. 14, pp. 1469–1476, Oct. 1999.

[3] P. Pillay and A. Bhattacharjee, "Application of wavelets to model short–term power system disturbances," *IEEE Trans. Power Delivery*, vol. 11, pp. 2031–2037, Oct. 1996.

[4] Rahim Abdullah, Abdul, et al. "Performance Evaluation of Real Power Quality Disturbances Analysis Using S-Transform." Applied Mechanics and Materials, vol. 752–753, Trans Tech Publications, Ltd., Apr. 2015, pp. 1343–1348. doi:10.4028/www.scientific.net/amm.752-753.1343.

[5] Beuter, C., Oleskovicz, M.: S-transform: from main concepts to some power quality applications. IET Signal Process. 14(3), 115–123 (2019).

[6] J. Ladan and Edward R. Vrscay," The Discrete Orthonormal Stockwell Transform and Variations, with Applications to Image Compression", ICIAR 2013, LNCS 7950, pp. 235–244, 2013.

[7] Drabycz, S., Stockwell, R.G., Mitchell, J.R.: Image texture characterization using the discrete orthonormal s-transform. Journal of Digital Imaging 22(6), 696–708 (2009).

[8] Jaya Bharata Reddy, M., Raghupathy, R. K., Venkatesh, K. P., & Mohanta, D. K. (2013). Power quality analysis using discrete orthogonal S-transform (DOST). Digital Signal Processing, 23(2), 616–626. http://dx.doi.org/10.1016/j.dsp.2012.09.013

[9] M. Jaya Bharata Reddy, B. Karthik Chandra, D.K. Mohanta, A DOST based approach for the condition monitoring of 11 kV distribution line insulators, IEEE Trans. Dielectr. Electr. Insul. 18 (2) (April 2011) 588–595.

[10] Seckin Karasu, Zehra Sarac," Investigation of power quality disturbances by using 2d discrete orthonormal s-transform, machine learning and multi-objective evolutionary algorithms Swarm Evol. Comput., 44 (2019), pp. 1060–1072. https://doi.org/10.1016/j.swevo.2018.11.002

[11] Xi Zhong Cui, Han Ping Hong; Use of Discrete Orthonormal S- Transform to Simulate Earthquake Ground Motions. *Bulletin of the Seismological Society of America* 2020; 110 (2): 565–575. doi: https://doi.org/10.1785/0120190212

[12] Cohen, L. (1995). Time-Frequency Analysis, Vol. 778, Prentice Hall, Upper Saddle River, New Jersey.

[13] A. A. Ahmad, A. Ehimen Airoboman, A. Abdulaziz and H. Hussaini, "Power Quality Disturbances Analysis using Two Forms of Wigner-Ville Distribution," 2019 IEEE PES/IAS Power Africa, Abuja, Nigeria, 2019, pp. 424–428, doi: 10.1109/PowerAfrica.2019.8928911.

[14] Wang, J.; Ye, N.; Ge, L. Steady-State Power Quality Synthetic Evaluation Based on the Triangular Fuzzy BW Method and Interval VIKOR Method. *Appl. Sci.* 2020, *10*, 2839. https://doi.org/10.3390/app10082839

[15] Martinez, R.; Castro, P.; Arroyo, A.; Manana, M.; Galan, N.; Moreno, F.S.; Bustamante, S.; Laso, A. Techniques to Locate the Origin of Power Quality Disturbances in a Power System: A Review. Sustainability 2022, 14, 7428. https://doi.org/10.3390/su14127428

[16] Gopal lal Rajora, Miguel A. Sanz-Bobi, Carlos Mateo Domingo,' Application of Machine Learning Methods for Asset Management on Power Distribution Networks', Emerging Science Journal, Vol. 6, No. 4, p. 905–920, 2022. DOI: http://dx.doi.org/10.28991/ESJ-2022-06-04-017]

[17] Muhammad Bilal Akhtar, 'The Use of a Convolutional Neural Network in Detecting Soldering Faults from a Printed Circuit Board Assembly', HighTech and Innovation Journal, Vol. 3, No. 1, 2022, p:1-14. http://dx.doi.org/10.28991/HIJ-2022-03-01-01

[18] R.G. Stockwell, A basis for efficient representation of the S-transform, Digital Signal Process. 17 (1) (2007) 371–393.

[19] S. Drabycz, R.G. Stockwell, J.R. Mitchell, Image texture characterisation using the discrete orthogonal S-transform, J. Digit. Imaging 22(6) (2009) 696–708.

[20] Xiao, Y.; Yang, H.; Liu, A. Short time disturbance detection using DCT analysis in distribution system. In Proceedings of the CIRED 2005-18th International Conference and Exhibition on Electricity Distribution, Turin, Italy, 6–9 June 2005.

[21] Imtiaz, H.; Sanam, T.F. Frequency domain feature extraction for power quality disturbance classification. In Proceedings of the 2013 International Conference on Informatics, Electronics and Vision, ICIEV 2013, Dhaka, Bangladesh, 17–18 May 2013.

[22] Hüseyin Eriști, Özal Yıldırım, Belkıs Eriști, Yakup Demir, 'Automatic recognition system of underlying causes of power quality disturbances based on S-Transform and Extreme Learning Machine, International Journal of Electrical Power & Energy Systems, Volume 61, 2014, pp. 553–562, https://doi.org/10.1016/j.ijepes.2014.04.010

[23] K. Thirumala, M. S. Prasad, T. Jain and A. C. Umarikar, "Tunable-Q Wavelet Transform and Dual Multiclass SVM for Online Automatic Detection of

Power Quality Disturbances," in IEEE Transactions on Smart Grid, vol. 9, no. 4, pp. 3018–3028, July 2018, doi: 10.1109/TSG.2016.2624313.

[24] H. I. Hussein, G, A. Salman and A. M. Ghadban "Employment of PSO Algorithm to Improve the Neural Network Technique for Radial Distribution System State Estimation", INTERNATIONAL JOURNAL ON SMART SENSING AND INTELLIGENT SYSTEMS, Vol. 12, Issue 1 (2019) pp. 1–10. DOI: 10.21307/ijssis-2019-005